PRAMANA
—journal of
physics

© Printed in India

Vol. 48, No. 1,
January 1997
pp. 303–323

Control of spatiotemporal chaos: A study with an autocatalytic reaction-diffusion system

NITA PAREKH, V RAVI KUMAR and B D KULKARNI
Chemical Engineering Division, National Chemical Laboratory, Pune 411 008, India

Abstract. The characterization of chaotic spatiotemporal dynamics has been studied for a representative nonlinear autocatalytic reaction mechanism coupled with diffusion. This has been carried out by an analysis of the Lyapunov spectrum in spatially *localised* regions. The linear scaling relationships observed in the invariant measures as a function of the *sub-system* size have been utilized to assess the controllability, stability and synchronization properties of the chaotic dynamics. The dynamical synchronization properties of this high-dimensional system has been analyzed using suitable Lyapunov functionals. The possibility of controlling spatiotemporal chaos for relevant objectives using available noisy scalar time-series data with simultaneous self-adaptation of the control parameter(s) has also been discussed.

Keywords. Spatiotemporal chaos; reaction-diffusion systems; autocatalysis; Lyapunov exponents; synchronization and control; parametric self-adaptation.

PACS Nos 05.70; 82.20; 47.54; 05.45

1. Introduction

Spatially extended nonlinear systems are known to exhibit a wide variety of complex dynamics ranging from stable stationary states to coherent travelling waves, solitons and spatiotemporal chaos. Studies on this topic have been reviewed by Cross and Hohenberg [1] from a global perspective and their importance in many physical, chemical, biological and social systems have been summarized. To cite a few examples, complex patterns have been experimentally observed in hydrodynamic fluids, nonlinear optics, crystallization of solids, chemically reacting systems, morphogenesis, self-replication of living cells, neural systems, population dynamics, and economics. Even though these systems are high-dimensional due to mechanisms such as diffusion, convection, etc., concurrently occurring in the spatial domain, a wide range of complex phenomena exhibited by these systems may be modelled by simple partial differential equations or coupled maps. Considerable application potential exists if it were possible to devise strategies that would regulate and control these dynamical patterns to exhibit the desired behaviour. This is especially true for systems exhibiting spatiotemporal chaotic patterns which are highly sensitive to the initial conditions and parameter settings [2] and their robust control needs highly efficient and newer techniques of analysis to be developed.

Systems exhibiting chaotic behaviour offer the advantage of controlling the system dynamics in a variety of dynamical patterns with low energy inputs [3]. Typically, an experimenter may wish to stabilize the spatiotemporally chaotic dynamics, or switch

it over to a different dynamical pattern (which may also be chaotic), using limited available information in the form of scalar time-series data in the spatial domain. Possible control strategies in such situations would require controllers to be dispersed in the spatial domain with each one perturbing the value of the chosen control parameter(s), or alternatively, introducing appropriate forcing in the form of dynamical waveforms from outside the system. Recent studies using these methodologies [4–7] have shown that it may be possible to suitably tune the spatiotemporally chaotic dynamics to a stabilized mode or a periodic orbit of the homogeneous system, devoid of spatial effects. A dense distribution of the controllers may be necessary to account for the large number of unstable degrees of freedom in high-dimensional systems. However, if some information about the basic mechanism governing the system dynamics is known, then ingenious strategies involving simple localized control algorithms may be employed. For instance, the spatiotemporal patterns observed in cardiac tissues [8], reaction-diffusion models for catalysis [9, 10], and Ginzburg-Landau equation [11–13] arise because of unstable topological defects nucleating spontaneously from an initial disordered state. In such situations it has been shown that the stabilization of even one wave-generating defect may interact and control all the others right up to the system boundary [13]. In the event when the spatiotemporal system is subjected to noise and a periodic forcing function, the cooperative effects that may arise between the inherent nonlinear dynamics, the external noise and periodic forces may stabilize the system dynamics due to the phenomenon of stochastic resonance. In fact, in a recent experimental study with linearly coupled array of nonlinear oscillators, it has been shown that ordered periodic states can be achieved by the optimization of noise levels and/or forcing frequency [14, 15]. Thus, while working with chaotic systems, even unconventional methods may be rationally applicable for regulating the system dynamics.

The control of nonlinear chaotic systems may also be looked at from a different viewpoint. Given a process from which we monitor scalar time-series data, can we use it to drive a response system so that its dynamics in all the other non-monitored variables becomes synchronized with that of the process? Despite the fact that the chaotic behaviour exhibits rapid decorrelation of nearby orbits, it has been observed that it may be possible to synchronize the response system dynamics to that of the process [16]. Considerable attention has been focussed on this topic in the recent years and conditions for obtaining synchronization have been studied when the response system is: 1) a replica of the process with incorrect knowledge of the initial conditions and 2) a non-replica of the process with unknown initial conditions and incorrect parameter settings. In particular it has been shown that for synchronization in initial conditions to occur, the response system, excluding the driving variables should possess only negative Lyapunov exponents [17–26]. When the response system is a non-replica of the process, synchronization may be possible by suitable perturbations in the response parameter(s) (depending upon local stability considerations) [27, 28] – much in the same fashion as suggested by OGY for controlling chaos [29, 30].

It may be noted that the above synchronization and control studies refer to systems described by low-dimensional chaotic systems. On the other hand, spatio-temporal chaotic systems may be thought of as a network of chaotic elements with a large number of positive Lyapunov exponents, and hence, for their dynamical synchronization a large

number of driving signals may be necessary. Furthermore, it would be computationally difficult to characterize the system dynamics and clearly demarcate the stable and unstable directions associated with the attractor because of the high dimensions involved [7, 31–33, 35, 37–39]. It is then worthwhile to see if simpler and practical ways of analyzing these systems can be devised. A possible strategy may be to first assess the complexity and stability properties of the high-dimensional system in a lower dimensional framework. Our earlier studies on this topic have shown that interesting scaling relationships in the system invariant measures (such as Lyapunov exponents, entropy, etc.) as a function of sub-system size exists for the spatiotemporally chaotic dynamics in nonlinear reaction-diffusion systems [40]. An analysis of these relationships may yield valuable information about the requirements of spatial time-series data for the characterization and control of spatiotemporal systems.

In this paper, we shall discuss the control of spatiotemporally chaotic dynamics in nonlinear reaction-diffusion systems for limitations in the knowledge of the system. The reaction-diffusion system considered here belongs to a fairly general class of chemically reacting systems involving nonlinearity by way of autocatalytic steps [45, 49] and in the following section we shall elaborate on the specifics of the system studied. Subsequently, in § 3 we summarize the possible methodology to characterize the spatiotemporal chaotic behaviour in terms of sub-system invariant measures like Lyapunov exponents, entropy, etc. Section 4 studies the synchronization and control of replica and non-replica response systems with simultaneous estimation of the response parameter(s) and § 5 briefly summarizes the scope of the results.

2. Model description

In recent times considerable interest has been aroused in the study of nonlinear reaction-diffusion systems with the experimental observance of complex spatiotemporal patterns, e.g., striped, hexagonal, travelling waves, and spatiotemporal chaos in a simple gel-reactor uncontaminated by convection effects [41, 44]. Pattern formation in these systems arises as a result of spontaneous symmetry breaking transitions with intrinsic length scales dependent on the diffusion coefficients and the reaction rate constants [42, 43]. An interesting class of spatial patterns observed include spots which have an uncanny resemblance to what is observed in many biological systems in the sense that they replicate, grow and die [46, 47]. These replicating patterns, do not have the high degree of sensitivity associated with the chaotic dynamics and hence their control is less difficult. In fact, in an earlier study with a simple autocatalytic reaction-diffusion model, using controllers dispersed in the spatial domain, we have shown that the control of these patterns in desired dynamical states may be possible [48]. In the present study we consider a similar reaction network with an additional mechanistic step involving a new species D, i.e., a three-step parallel autocatalytic reaction mechanism [49] with competing interactions between the chemical species A, D, and B, viz.,

$$A + 2B \longrightarrow 3B, \quad r_1 = k_1 C_A C_B^2, \tag{I}$$

$$D + 2B \longrightarrow 3B, \quad r_2 = k_2 C_D C_B^2, \tag{II}$$

$$B \longrightarrow C, \quad r_3 = k_3 C_B, \tag{III}$$

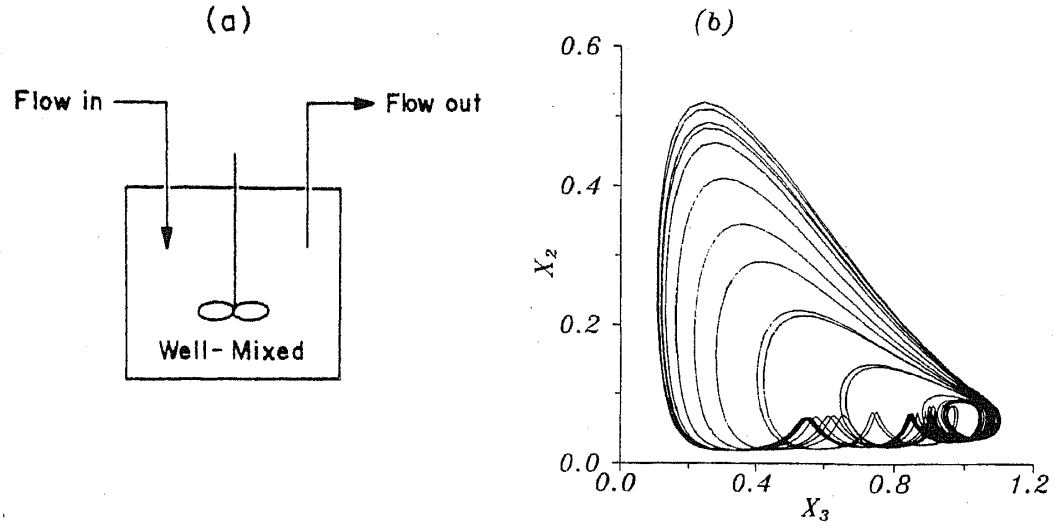

Figure 1. (a) Schematic diagram of a well-mixed continuous stirred tank reactor (CSTR). (b) Temporal chaos arising for the autocatalytic reaction (1) in a CSTR, shown as a phase-plane plot; $\alpha = 1.5$; $\beta = 2.93$; $Da_1 = 18000$; $Da_2 = 400$; $Da_3 = 80$.

and the rate expressions r_i, $i = 1, 2, 3$ for each step, given alongside. Nonlinear feedback in this mechanism occurs due to the rates of formation of species B being autocatalytic in steps (I) and (II), while, in (III) the effect is inhibitory. For a continuous flow well-mixed cell (shown in figure 1a), the model description for the above reaction takes the following dimensionless form

$$\frac{dX_1}{dt} = 1 - X_1 - Da_1 X_1 X_3^2,$$

$$\frac{dX_2}{dt} = \beta - X_2 - Da_2 X_2 X_3^2,$$

$$\frac{dX_3}{dt} = 1 - (1 + Da_3)X_3 + \alpha(Da_1 X_1 + Da_2 X_2)X_3^2, \tag{1}$$

where X_i, $i = 1, 2, 3$, respectively, represent the dimensionless species concentrations of A, D, and B relative to their concentrations at the inlet to the cell. Here, Da_i's are the dimensionless kinetic parameters associated with the reaction steps (I–III) and the parameters α and β are the feed concentration ratios of species B and D with respect to A. An analysis of the dynamical properties of this cell shows features such as multi-stationarity, oscillatory behaviour and chaos in chosen parameter space of α, β and Da_i's [49]. In figure 1b a typical phase portrait diagram of X_2 vs X_3 depicting the chaotic dynamical behaviour of (1) (with maximum Lyapunov exponent, $\lambda_{max} \sim 1.36$) is shown. On introducing a diffusive transport mechanism for a system of N coupled autocatalators (1), the system dynamics may be described by the following set of PDE's, viz.,

$$\frac{\partial X_1(\mathbf{r}, t)}{\partial t} = 1 - X_1(\mathbf{r}, t) - Da_1 X_1(\mathbf{r}, t) X_3^2(\mathbf{r}, t) + d_1 \frac{\partial^2 X_1(\mathbf{r}, t)}{\partial \mathbf{r}^2}$$

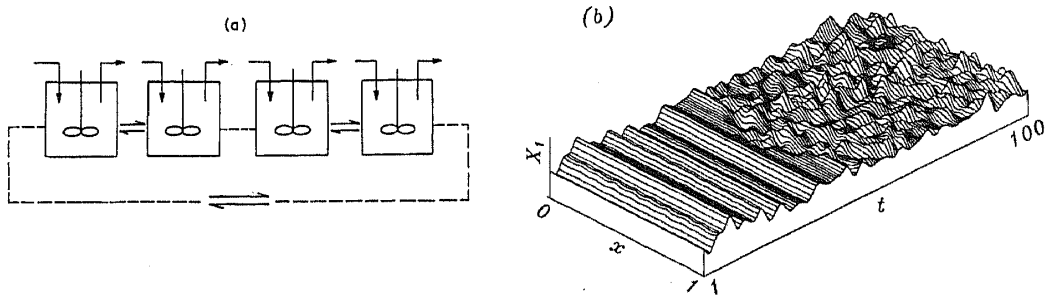

Figure 2. (**a**) Schematic of N CSTRs coupled bi-directionally via diffusion in one spatial dimension with periodic boundary conditions. (**b**) Spatiotemporal chaos arising for a perturbation given at $t = 40$. $D_1 = D_2 = 1.0$; $D_3 = 0.01$; $\alpha = 1.5$; $\beta = 2.93$; $Da_1 = 18000$; $Da_2 = 400$; $Da_3 = 80$; [X_1 axis-scale: (0.0, 0.07).

$$\frac{\partial X_2(\mathbf{r},t)}{\partial t} = \beta - X_2(\mathbf{r},t) - Da_2 X_2(\mathbf{r},t) X_3^2(\mathbf{r},t) + d_2 \frac{\partial^2 X_2(\mathbf{r},t)}{\partial \mathbf{r}^2}$$

$$\frac{\partial X_3(\mathbf{r},t)}{\partial t} = 1 - (1 + Da_3) X_3(\mathbf{r},t) + \alpha [Da_1 X_1(\mathbf{r},t) + Da_2 X_2(\mathbf{r},t)] X_3^2(\mathbf{r},t) + d_3 \frac{\partial^2 X_3(\mathbf{r},t)}{\partial \mathbf{r}^2}, \tag{2}$$

where $\mathbf{r} \equiv (x, y, z)$ is the spatial vector; and d_i, $i = 1, 2, 3$ are the dimensionless diffusion coefficients of the respective species A, D and B. Autocatalytic reaction-diffusion systems of the type (2) are known to possess a rich variety of dynamical patterns with properties such as excitability, wave reflection and wave splitting, propagating fronts, etc. [50, 51].

In this paper, all studies were carried out for N independent autocatalators coupled via bi-directional diffusion on a one-dimensional spatial lattice (schematically shown in figure 2a). On Euler discretizing the Laplacian, $\partial^2/\partial x^2$, in the spatial dimension x, viz., we obtain

$$\frac{\partial X_1(j,t)}{\partial t} = 1 - X_1(j,t) - Da_1 X_1(j,t) X_3^2(j,t) + D_1 [X_1(j+1,t) - 2X_1(j,t) + X_1(j-1,t)],$$

$$\frac{\partial X_2(j,t)}{\partial t} = \beta - X_2(j,t) - Da_2 X_2(j,t) X_3^2(j,t) + D_2 [X_2(j+1,t) - 2X_2(j,t) + X_2(j-1,t)],$$

$$\frac{\partial X_3(j,t)}{\partial t} = 1 - (1 + Da_3) X_3(j,t) + \alpha [Da_1 X_1(j,t) + Da_2 X_2(j,t)] X_3^2(j,t) + D_3 [X_3(j+1,t) - 2X_3(j,t) + X_3(j-1,t)], \tag{3}$$

with $D_i = d_i/(\Delta x)^2$, Δx being the spatial mesh size; $j = 1, 2, \ldots, N$. The number of degrees of freedom is significantly increased to $3N$ and the characterization of the system dynamics is, now, not a trivial task. In this study, the diffusion coefficients of the species A and D are assumed equal throughout and much greater than that for the species B, i.e., $D_1 = D_2 > D_3$. The unequal rates of diffusion and the local nonlinearity may then result

in the formation of complex spatiotemporal patterns including spatiotemporal chaos depending on the parameter values. In figure 2b is shown the spatiotemporally chaotic dynamics exhibited by (3) for $N = 64$ and assuming periodic boundary conditions. Initially, all the N cells were assigned identical initial conditions and the parameter values were chosen corresponding to single cell (1) exhibiting chaotic dynamics (figure 1b). The extended system (3) was then simulated using the fourth order Runge–Kutta algorithm with time step $\Delta t = 0.0002$. For time $t < 40$ (in dimensionless units), the system dynamics is seen to be spatially correlated though temporally it is uncorrelated and chaotic. Note that the diffusion mechanism is not active in this region because of identical initial conditions assumed over the entire spatial domain, and therefore all the cells evolve synchronously. Now at time $t = 40$, a perturbation was given to the set of eleven cells lying in the central region of the lattice. This perturbation assumed that the dynamics of the chosen cells progressively went out of phase with each other by time $t = 0.002$. A spread of this perturbation to the system boundaries by diffusion, with a complete loss in the spatial correlation, is qualitatively seen in figure 2b and this dynamical behaviour was seen to persist indefinitely. Characterization of this loss in correlation and their effects, however, need to be studied quantitatively to make more meaningful interpretations. The following section discusses a means of doing so.

3. Characterization of reaction-diffusion dynamics

The characterization of spatiotemporal dynamics in terms of the Lyapunov exponents [52] which quantify the growth rate of trajectories for infinitesimally small perturbations will be discussed in this section. For the spatially discretized system (3) with three chemical species interacting on a one-dimensional lattice of size N, there are $3N$ dependent variables. Hence the complete Lyapunov spectrum would have $3N$ exponents and their calculation would be computationally very intensive, especially for large N. To alleviate this difficulty, in an earlier study we discussed the analysis of the Lyapunov spectrum for sub-systems of size $n_s (\ll N)$ and studied the behaviour of the system invariants as $n_s \to N$ [40]. For the sake of completeness in discussing issues related to the control of these systems, we shall now review this approach, highlighting the major results obtained.

For the extended system (3) with κ denoting the set of fixed parameters, the temporal evolution of the concentrations of each of the species for chosen values of D_i may be functionally written as

$$\frac{dX_i(k,t)}{dt} = F_{i,k}(X_1(k,t), \ldots, X_3(k,t), X_i(k \pm 1, t), \kappa), \tag{4}$$

where the first index $i = 1, 2, 3$ of the functionals $F_{i,k}$ denotes the respective species and the second index $k = 1, \ldots, n_s$ represents a sub-system lattice site. The Lyapunov exponents of the sub-system of size n_s may then be calculated in a manner similar to that for the full system [52], viz.,

$$\lambda_l^{(s)} = \lim_{t \to \infty} \sup \frac{1}{t} \ln \frac{| \delta \mathbf{X}^l(t) |}{| \delta \mathbf{X}^l(t_0) |}, \quad l = 1, \ldots, 3n_s, \tag{5}$$

where $\delta \mathbf{X}^l(t_0)$ refers to the infinitesimal perturbation from a reference state at $t = t_0$ and $\delta \mathbf{X}^l(t)$ its evolution at a time t. While calculating these exponents for (4), open boundary conditions were assumed at the sub-system boundary sites, i.e., at $k = 1$ and $k = n_s$. The open boundary conditions indicate that only for the purposes of evaluating the λ_l's, the flow of information from the outer site of the sub-system boundaries, may be likened, to presence of noise in the analysis. Alternatively, for the 1d lattice, we may characterize the sub-system dynamics on excluding the outermost sub-system boundary sites, although time-series signals at these boundary sites are available. The effective sub-system size for characterization is now $n_s - 2$, and the invariant measures of (4) can be studied accurately.

The characterization of the sub-system dynamics may now be carried out by applying the well-known Kaplan and Yorke (KY) conjecture [53] to the spectrum of sub-system Lyapunov exponents, $\lambda_l^{(s)}$. For doing so, we define the effective sub-system Lyapunov dimension, $d_L^{(s)}$, as

$$d_L^{(s)} = l + \frac{1}{|\lambda_{l+1}^{(s)}|} \sum_{i=1}^{l} \lambda_i^{(s)}, \tag{6}$$

where l is the largest integer for which the sum of the exponents, $\lambda_1^{(s)} + \cdots + \lambda_l^{(s)} \geq 0$. If $\lambda_1 < 0$, then $d_L^{(s)} = 0$ and if $l = 3n_s$, then $d_L^{(s)} = 3n_s$ [54]. Further reduction in the computational effort is possible as it may not be necessary to evaluate all the $3n_s$ sub-system exponents. A relationship in the variation of $d_L^{(s)}$ with n_s would then help in establishing the number of effective variables required to determine the long-term behaviour of the complete system dynamics. From a knowledge of $d_L^{(s)}$ we can define the sub-system dimension density, $\rho^{(s)}$, as

$$\rho^{(s)} = \frac{d_L^{(s)}}{n_s}, \tag{7}$$

by normalizing the sub-system Lyapunov dimension with its size n_s. The behaviour of $\rho^{(s)}$ as a function of n_s may then importantly help in identifying a critical sub-system size, n_{sc}, required for accurate characterization of the complete system dynamics.

Another important invariant measure is the Kolmogorov–Sinai (KS) entropy used for quantifying the mean information production and the growth of uncertainty in a system subjected to small perturbations [53]. The KS entropy is defined as the sum of the positive Lyapunov exponents λ_+ [52, 55]. For regular predictable behaviour, the KS entropy is zero while for chaotic systems it takes a finite positive value and tends to infinity for a stochastic process. In the present analysis we shall use this relationship for evaluating the sub-system KS-entropy, $h^{(s)}$, as

$$h^{(s)} = \sum \lambda_+^{(s)}, \tag{8}$$

and the normalized sub-system entropy, $\langle h^{(s)} \rangle$, as

$$\langle h^{(s)} \rangle = \sum \lambda_+^{(s)} / n_s. \tag{9}$$

We now discuss the role of these sub-system invariants in the characterization of the full spatiotemporal system. In figure 3a is shown a plot of the sub-system dimension

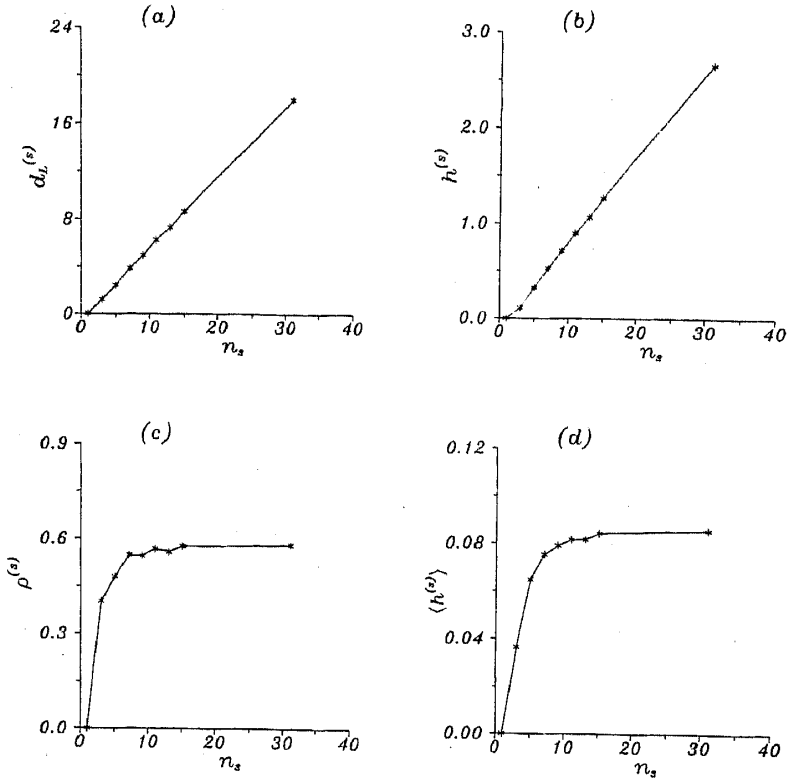

Figure 3. Behavior of the sub-system invariants as a function of its size n_s: (**a**) Lyapunov dimension, $d_L^{(s)}$; (**b**) entropy, $h^{(s)}$; (**c**) dimension density $\rho^{(s)}$; (**d**) normalized entropy, $\langle h^{(s)} \rangle$.

$d_L^{(s)}$ as a function of its size n_s. A clear linear scaling relationship in the sub-system dimension is seen for increasing sub-system size (figure 3a). This suggests that it may indeed be possible to determine the effective dimensionality of the whole system from an analysis of a relatively small sub-system. Some generic conjectures based on dimensionality have also been seen [34]. A clear linear scaling relationship with increasing sub-system size was also observed for the sub-system KS entropy, $h^{(s)}$, shown in figure 3b. The sub-system dimension density, $\rho^{(s)}$, is however, seen to saturate to a constant value for n_s greater than a critical sub-system size n_{sc} (figure 3c). This converging behaviour of $\rho^{(s)}$ for $n_s > n_{sc}$, may importantly help in assessing the number of degrees of freedom required for the characterization of the whole system. The saturating behaviour observed for the normalized sub-system entropy, $\langle h^{(s)} \rangle$, (figure 3d) suggests that even though the total entropy of the sub-system may increase with its size, the average rate of information loss/gain levels off for $n_s > n_{sc}$. These results suggest that sub-system analysis may suffice for the characterization of the full system dynamics. Similar scaling relationships in the system invariants as a function of sub-system size have also been observed for coupled maps with near neighbour interactions indicating possible generalizations [35, 36]. The knowledge of these sub-system properties may be used in identifying favourable conditions for controlling the spatiotemporal system and in the following section we shall further elaborate on this aspect.

4. Synchronization and control of spatiotemporal chaos

In this section, we discuss the synchronization and control of the spatiotemporally chaotic dynamics of a response system driven by monitored time-series signals from a spatiotemporal process for various objectives like stabilizing the chaotic behaviour of the response system and its ability to mimic the process dynamics under different situations [16]. In practice, there exists constraints in the monitoring of scalar time-series data from the entire spatial domain of the process, and moreover, this data may generally be noisy due to errors arising during measurement. It would be desirable to consider the control of the spatiotemporal dynamics of replica and non-replica response systems for these limitations.

4.1 *Synchronization in replica systems*

To begin with, we first consider the response system to be a replica of a spatiotemporally chaotic process, i.e., the response and the process systems are assumed to be identical in all respects except in their initial conditions, $X_i(j,0) \neq \hat{X}_i(j,0)$, where $\hat{X}_i(j,0)$ denote the response system variables. The response system model may then be written in its variables, $\hat{X}_i(j,t)$, as

$$\begin{aligned}
\dot{\hat{X}}_1(j,t) &= F_1(\hat{X}_1(j,t),\hat{X}_3(j,t)) \\
&= 1 - \hat{X}_1(j,t) - Da_1\hat{X}_1(j,t)\hat{X}_3^2(j,t) \\
&\quad + D_1[\hat{X}_1(j+1,t) - 2\hat{X}_1(j,t) + \hat{X}_1(j-1,t)], \\
\dot{\hat{X}}_2(j,t) &= F_2(\hat{X}_2(j,t),\hat{X}_3(j,t)) \\
&= \beta - \hat{X}_2(j,t) - Da_2\hat{X}_2(j,t)\hat{X}_3^2(j,t) \\
&\quad + D_2[\hat{X}_2(j+1,t) - 2\hat{X}_2(j,t) + \hat{X}_2(j-1,t)], \\
\dot{\hat{X}}_3(j,t) &= F_3(\hat{X}_1(j,t),\hat{X}_2(j,t),\hat{X}_3(j,t)) \\
&= 1 - (1+Da_3)\hat{X}_3(j,t) + \alpha[Da_1\hat{X}_1(j,t) + Da_2\hat{X}_2(j,t)]\hat{X}_3^2(j,t) \\
&\quad + D_3[\hat{X}_3(j+1,t) - 2\hat{X}_3(j,t) + \hat{X}_3(j-1,t)],
\end{aligned} \tag{10}$$

where, $j = 1,2,\ldots,N$. If the response system (10) is now assumed to be driven by scalar time-series signals, $X_3(j,t)$, $j = 1,2,\ldots,N$, from the process, its dynamics follow

$$\begin{aligned}
\dot{\hat{X}}_1(k,t) &= F_1(\hat{X}_1(k,t),X_3(k,t)), \\
\dot{\hat{X}}_2(k,t) &= F_2(\hat{X}_2(k,t),X_3(k,t)), \\
\dot{\hat{X}}_3(k,t) &= F_3(\hat{X}_1(k,t),\hat{X}_2(k,t),X_3(j,t)),
\end{aligned} \tag{11}$$

and was found to completely synchronize with the process dynamics, in all the $3N$ variables. This is clearly seen in figure 4a from the diminishing behaviour of the relative error in the response and process dynamics, i.e., $e_2'(j,t) = [\hat{X}_2(j,t) - X_2(j,t)]/X_2(j,t) \to 0$. (Similar synchronized behaviour was observed in the other two variables also).

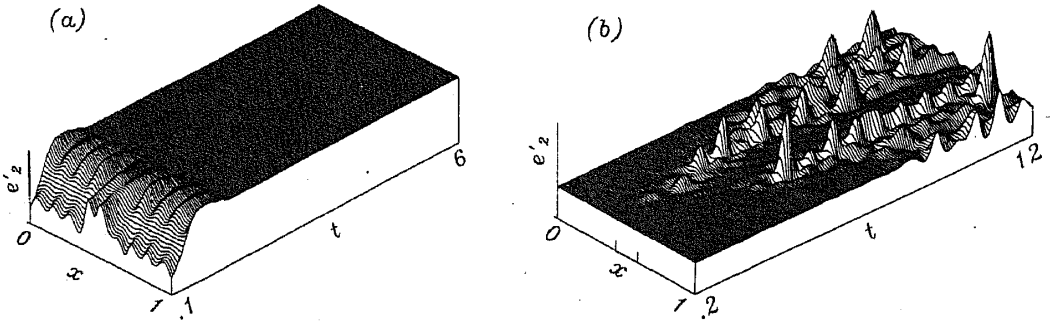

Figure 4. Synchronization in a replica system for parameter values in figure 2. The relative space-time error behaviour for $e_2'(j,t)$ shown. (**a**) Complete synchronization in the spatio-temporally chaotic dynamics of the response system obtained on using driving signals, $X_3(j,t)$, $j=1,\ldots,N$, from the process; e_2' axis-scale: $(-0.005, 0.0007)$. (**b**) On using sub-system driving signals, $X_3(k,t)$, $k=1,\ldots,n_s$, for $n_s=11$, from the central region (shown by tics), synchronization was observed only within the sub-system. e_2' axis-scale: $(-1.11, 6.35)$.

We now show that it may be possible to explain the observed synchronization behaviour of the combined response-process dynamics using Lyapunov stability analysis. The method suggests that a given system is stable, if any continuously derivable positive definite function, L, (called the Lyapunov function) can be defined along a trajectory with the property that its time derivative, $\dot{L} \leq 0$, as $t \to \infty$ [56]. This method may be advantageously used since it affords analytical reasoning of the stability properties of the system. In the present study, we show by constructing suitable Lyapunov functionals in terms of error variables, $e_i(j,t) = \hat{X}_i(j,t) - X_i(j,t)$, that synchronization in the dynamics between the response and the process may be assessed. The dynamical equations for the error function variables $e_i(j,t)$ are

$$\begin{aligned}\dot{e}_1(j,t) &= \dot{\hat{X}}_1(j,t) - \dot{X}_1(j,t) \\ &= -e_1(j,t)[1 + Da_1 X_3^2(j,t)] \\ &\quad + D_1[e_1(j-1,t) - 2e_1(j,t) + e_1(j+1,t)], \qquad (12)\\ \dot{e}_2(j,t) &= \dot{\hat{X}}_2(j,t) - \dot{X}_2(j,t) \\ &= -e_2(j,t)[1 + Da_2 X_3^2(j,t)] \\ &\quad + D_2[e_2(j-1,t) - 2e_2(j,t) + e_2(j+1,t)], \qquad (13)\\ \dot{e}_3(j,t) &= \dot{\hat{X}}_3(j,t) - \dot{X}_3(j,t) \\ &= \alpha[Da_1 e_1(j,t) + Da_2 e_2(j,t)]X_3^2(j,t), \qquad (14)\end{aligned}$$

written using (3) and (10). Then, for a chosen positive Lyapunov functional L defined as $L = \sum_i \sum_j e_i^2(j,t)$, its derivative $\dot{L}$ is

$$(1/2)\dot{L} = \sum_{i=1}^{3} \sum_{j=1}^{N} e_i(j,t)\dot{e}_i(j,t). \qquad (15)$$

Substituting (12–14) in (15) and for the assumed periodic boundary conditions, we obtain

on simplification

$$\sum_{j=1}^{N} e_1(j,t)\dot{e}_1(j,t) = -\sum_{j=1}^{N} {e_1}^2(j,t)[1 + Da_1 X_3^2(j,t)] - D_1 \sum_{j=1}^{N} [e_1(j,t) - e_1(j+1,t)]^2, \tag{16}$$

$$\sum_{j=1}^{N} e_2(j,t)\dot{e}_2(j,t) = -\sum_{j=1}^{N} {e_2}^2(j,t)[1 + Da_2 X_3^2(j,t)] - D_2 \sum_{j=1}^{N} [e_2(j,t) - e_2(j+1,t)]^2, \tag{17}$$

$$\sum_{j=1}^{N} e_3(j,t)\dot{e}_3(j,t) = \alpha \sum_{j=1}^{N} \{e_3(j,t)[Da_1 e_1(j,t) + Da_2 e_2(j,t)]X_3^2(j,t)\}. \tag{18}$$

It may be noted from (12) and (13) that the error dynamics of $e_1(j,t)$ and $e_2(j,t)$ are dependent only on their respective error function variables, and on the square of the driving signals, $X_3(j,t)$. Equations (12) and (13) are decoupled in this sense and may be considered independently for assessing the synchronization behaviour of $\hat{X}_1$ and $\hat{X}_2$ by independent Lyapunov functions $L_i = \sum_j e_i^2(j,t)$, $i = 1, 2$. Then, from (16) and (17), it is clear that the $\dot{L}_i$'s are negative definite, and $e_1(j,t), e_2(j,t) \to 0$ as $t \to \infty$ by the Lyapunov stability theorem. Using these conditions in (15), $\dot{L}$ is strictly nonpositive and indicates the stable convergence of the error dynamics (12–14) to the origin. That is, the response system would dynamically synchronize with the process dynamics in all its variables.

On the other hand, if the time-series signals are available from a sub-system of size $n_s (\ll N)$, then following the above Lyapunov stability analysis, synchronization should be possible only within the sub-system region. This is because for the variables outside the sub-system, the error function variables are governed by

$$\dot{e}_1(l,t) = -e_1(l,t) - Da_1[\hat{X}_1(l,t)\hat{X}_3^2(l,t) - X_1(l,t)X_3^2(l,t)] + D_1[e_1(l-1,t) - 2e_1(l,t) + e_1(l+1,t)], \tag{19}$$

$$\dot{e}_2(l,t) = -e_2(l,t) - Da_2[\hat{X}_2(l,t)\hat{X}_3^2(l,t) - X_2(l,t)X_3^2(l,t)] + D_2[e_2(l-1,t) - 2e_2(l,t) + e_2(l+1,t)], \tag{20}$$

$$\begin{aligned}\dot{e}_3(l,t) = {} & -(1 + Da_3)[\hat{X}_3(l,t) - X_3(l,t)] \\ & + \alpha Da_1[\hat{X}_1(l,t)\hat{X}_3^2(l,t) - X_1(l,t)X_3^2(l,t)] \\ & + \alpha Da_2[\hat{X}_2(l,t)\hat{X}_3^2(l,t) - X_2(l,t)X_3^2(l,t)] \\ & + D_3[e_3(l-1,t) - 2e_3(l,t) + e_3(l+1,t)],\end{aligned} \tag{21}$$

where l denotes the lattice sites outside the sub-system, i.e., $l = 1, 2, \ldots, N$, excluding the n_s sub-system lattices sites from the central region. Note that the terms (19) and (20) are now not necessarily negative and synchronization in these variables cannot be guaranteed.

This behaviour was numerically observed on driving the response system (10) by scalar time-series signals from a sub-system of the process of size $n_s = 11$, from the central region of the lattice. The space-time plot of the error function $e_2'(j,t)$ in figure 4b clearly shows only sub-system synchronization.

In situations when a suitable Lyapunov functional cannot be constructed, the synchronization capability of the response system with that of the process may be inferred from an analysis of the conditional Lyapunov exponents of the response system [18, 19]. Following the results of the sub-system invariants discussed in § 3, it may be sufficient to analyse the conditional Lyapunov exponents of only a sub-system of size $n_s(> n_{sc})$ of the response system. The procedure for calculating the conditional Lyapunov exponents of a sub-system is similar to that of the sub-system Lyapunov exponents discussed in the § 3, but now we need to monitor the growth rate of only $2n_s$ sets of orthonormal vectors $(\delta X_i(k,t),\ i = 1,2;\ k = 1,2,\ldots,n_s)$ in a linearized region of (11). The maximum conditional Lyapunov exponent for a sub-system of size $n_s = 11$ of the response system (11) was found to be negative ($\lambda_{max} \sim -0.07$), as expected. Thus, the sub-system conditional exponents may be used to assess the synchronization capability of the response system (see figure 4a).

4.2 *Synchronization in non-replica systems*

Next, we consider the situation when the response system is a non-replica of the process, i.e., the response and the process are assumed to be operating in different parametric regimes. Synchronization of the response dynamics with that of the process in this situation may be difficult because of inaccuracies in its parameter values. For example, consider both the process and the response system exhibiting spatiotemporal chaos, but with a chosen control parameter, β, of the process having a value 2.93 (which may not be known *a priori* in a given experimental situation), and the corresponding response parameter, $\hat{\beta}$, set incorrectly at 2.73 at $t = 0$. The hence response and the process evolve asynchronously because of this parametric inaccuracy, and simple driving as employed in subsection 4.1 for replica systems, was found to be insufficient for the complete dynamical synchronization. There exists a need, therefore, to correctly estimate the parametric inaccuracy. To do so, we focus attention on a convenient strategy which allows to correctly estimate the inaccuracy in the control parameter via suitably chosen functional forms for parametric self-adaptation. For low-dimensional chaotic systems it has been shown that many simple choices of the functional forms may indeed be used for parametric self-adaptation and control [57–65].

For parametric self-adaptation of spatiotemporal systems, we begin by introducing space-time dependence in the chosen response parameter, i.e., $\hat{\beta}(j,t)$ and define a new variable, $\Delta\beta(j,t)$, denoting the time-dependent parametric corrections to be made such that, $\hat{\beta}(j,t) = [\hat{\beta}(j,0) + \Delta\beta(j,t)] \to \beta$ as $t \to \infty$. For convenience, it was assumed that at $t = 0$, $\hat{\beta}(j,0) = \hat{\beta}$, and $\Delta\beta(j,0) = 0$, for $j = 1,2,\ldots,N$ with the following simple functional form for the dynamical corrections, $\Delta\beta(j,t)$, viz.,

$$\frac{d\Delta\beta(j,t)}{dt} = -[\hat{X}_3(j,t) - X_3(j,t)] = -e_3(j,t). \tag{22}$$

It would be interesting to see if a Lyapunov functional can predict the stability of the error

dynamics with the parametric self-adapter equation (22). The error dynamics in this case follows

$$\dot{e}_1(j,t) = -e_1(j,t)[1 + Da_1 X_3^2(j,t)] + D_1[e_1(j-1,t) - 2e_1(j,t) + e_1(j+1,t)], \tag{23}$$

$$\dot{e}_2(j,t) = (\hat{\beta}(j,0) + \Delta\beta(j,t)) - \beta - e_2(j,t)[1 + Da_2 X_3^2(j,t)] + D_2[e_2(j-1,t) - 2e_2(j,t) + e_2(j+1,t)], \tag{24}$$

$$\dot{e}_3(j,t) = \alpha[Da_1 e_1(j,t) + Da_2 e_2(j,t)]X_3^2(j,t). \tag{25}$$

It may be noted that, similar to the analysis for the replica system, the error dynamics of $e_1(j,t)$ is again dependent only on $e_1(j,t)$ and the square of the time-series signals, $X_3^2(j,t)$. That is, we can define a Lyapunov function $L_1 = \sum_j e_1^2(j,t)$ such that

$$(1/2)\dot{L}_1 = \sum_{j=1}^{N} e_1(j,t)\dot{e}_1(j,t) = -\sum_{j=1}^{N} e_1^2(j,t)[1 + Da_1 X_3^2(j,t)] - D_1 \sum_{j=1}^{N} [e_1(j,t) - e_1(j+1,t)]^2 \tag{26}$$

is negative definite. Hence, following the Lyapunov stability theorem, $e_1(j,t) \to 0$, irrespective of the dynamical behaviour of the time-series signals, $X_3(j,t)$ and the remaining variables of the response system. This implies that synchronization in $\hat{X}_1(j,t)$ is guaranteed and this feature may be used for studying the synchronization behaviour with respect to the remaining variables. Thus, on defining a positive Lyapunov functional of the form $L = \sum_j e_1^2(j,t) + e_1^2(j,t)[e_2^2(j,t) + e_3^2(j,t) + \Delta\beta^2(j,t)]$, we find that its derivative, $\dot{L}$, is strictly nonpositive as $t \to \infty$. Hence, dynamical synchronization of the response system with that of the process is likely with the corrections, $\Delta\beta(j,t)$, appropriately estimated. A numerical study confirmed the above prediction (results not shown).

It is interesting to note that the above Lyapunov functional analysis is valid even if the monitored time-series signals are noisy due to measurement errors. That is, we assume the response model to be driven by noisy scalar time-series data, $X_3'(j,t)$, of the form

$$X_3'(j,t) = X_3(j,t) + \gamma\eta(j,t), \quad j = 1,\ldots,N, \tag{27}$$

where γ is the intensity of Gaussian noise, $\eta(j,t)$. The inherent tendency of the response to reduce the errors $e_i(j,t)$, $i = 1,2,3$ still persists with a noise reduction capability depending on the noise level and frequency. Our studies showed that when the driving signals $X_3'(j,t)$, were assumed to be available from all the lattice sites, synchronization in the response variables was observed over the entire spatial domain even for noisy time-series signals. This is depicted in figures 5a and b, by the diminishing behaviour of the relative error signals $e_i'(j,t) = [\hat{X}_i(j,t) - X_i(j,t)]/X_i(j,t)$, $i = 1,2$, with the convergence of $\Delta\beta(j,t)$ to the mean correction, $\beta - \hat{\beta}(j,0) = 0.2$, shown in figure 5c. Note that $\Delta\beta(j,t)$ fluctuates around this mean correction in an attempt to filter the effects of noise on the dynamics of the response system. In keeping with the observations made earlier on studying synchronization properties for data monitored from a subsystem, the results obtained with noisy driving signals from a sub-system, i.e., $X_3'(k,t)$,

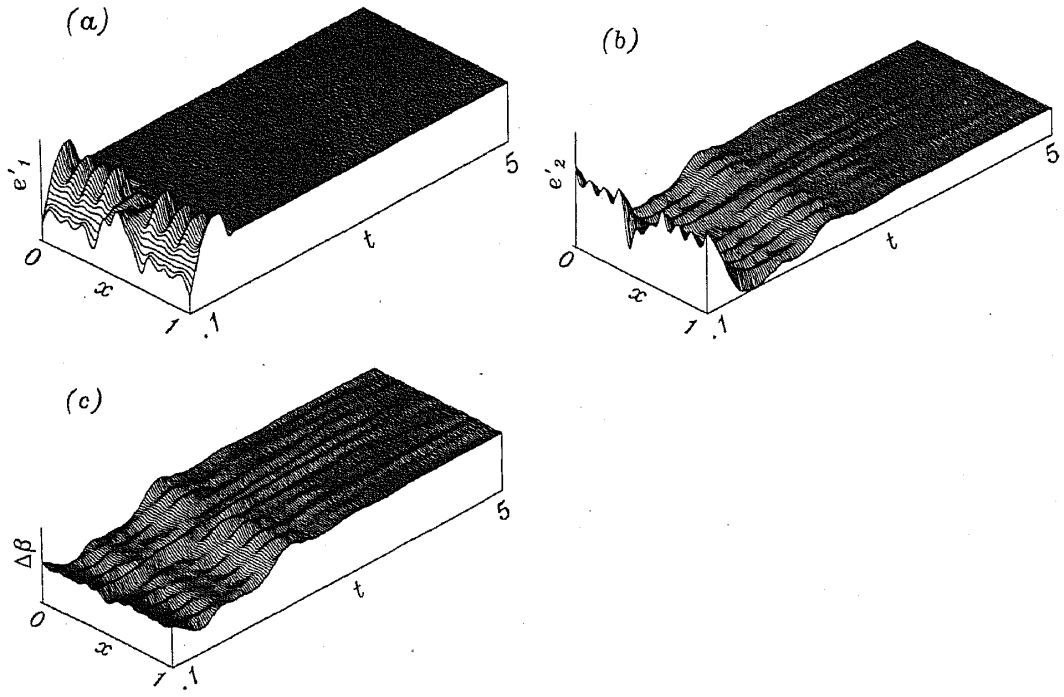

Figure 5. Synchronization in a non-replica system for an initial inaccuracy in response parameter $\hat{\beta}$, i.e., $\hat{\beta} = 2.73$, while process parameter $\beta = 2.93$. The study assumed the response system to be driven by time-series signals, $X'_3(j,t)$, $j = 1,2,\ldots,N$, corrupted with measurement noise of intensity $\gamma = 0.00002$. **(a, b)** The relative error signals, $e_1(j,t), e_2(j,t) \to 0$, showing the synchronization of the response dynamics with the process; e'_1 axis-scale: $(-0.051, 0.316)$; e'_2 axis-scale: $(-0.051, 0.316)$. (c) Space-time behaviour of the correction, $\Delta\beta(j,t)$, converging accurately to 0.2 over the entire spatial domain is seen; $\Delta\beta$ axis-scale: $(-0.051, 0.251)$.

$k = 1,2,\ldots,n_s$ showed that synchronization was again possible only within the sub-system region. This is shown in figures 6a and b, where the relative synchronization error, $e'_i(j,t)$, $i = 1,2$, has been plotted. Note that for the lattice sites outside the sub-system (and not covered by the adapter equations (22)), an average adaptation $\langle\Delta\beta\rangle = \sum_k \Delta\beta(k,t)/n_s$ was employed. The dynamical convergence of this average correction, $\langle\Delta\beta\rangle$, to 0.2 is shown in figure 6c. These results suggest that even with limited and inaccurate sub-system information, it may be possible to correctly estimate the inaccuracy in the chosen control parameter, though, complete dynamical synchronization of the response in all its variables may be a difficult task.

4.3 *Stabilization of spatiotemporal chaos*

Frequently, it may be necessary to stabilize the spatiotemporally chaotic dynamics and in this subsection we present the results obtained on driving a response system using limited and noisy time-series signals from a process exhibiting time-independent stable dynamics. The response system was assumed to exhibit spatiotemporal chaos with $\hat{D}a_3 = 80$ and the aim was to self-adapt this parameter so that the response system now self-regulates itself to operate at a desired stable state (say, at $Da_3 = 30$, not known

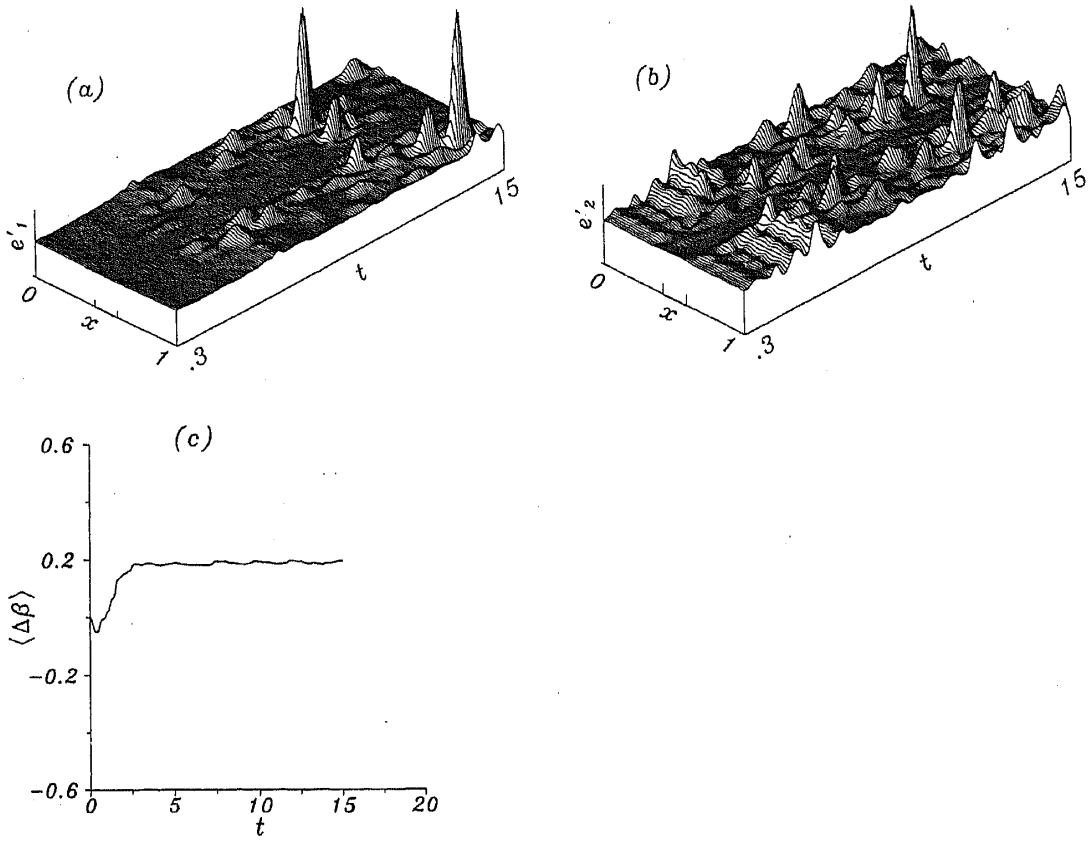

Figure 6. Synchronization behaviour of a spatiotemporally chaotic dynamics of the response when driven with noisy data from a sub-system of size $n_s = 11$, from the central region of the lattice. (**a, b**) Synchronization observed only within the sub-system region where, $e_1(j,t), e_2(j,t) \to 0$; e'_1 axis-scale: $(-24.89, 182.8)$; e'_2 axis-scale: $(-1.117, 8.316)$. (**c**) The temporal behaviour of $\langle\Delta\beta\rangle$, is seen to accurately estimate the correction required.

a priori). Thus, in this case, we study the inverse problem of locating the control parameter value which yields a desired output in the dependent variables of the response system. The dynamical equations for the error functions $e_i(j,t)$, in this situation follows

$$\dot{e}_1(j,t) = -e_1(j,t)[1 + Da_1 X_3^2(j,t)] + D_1[e_1(j-1,t) - 2e_1(j,t) + e_1(j+1,t)], \tag{28}$$

$$\dot{e}_2(j,t) = -e_2(j,t)[1 + Da_2 X_3^2(j,t)] + D_2[e_2(j-1,t) - 2e_2(j,t) + e_2(j+1,t)], \tag{29}$$

$$\dot{e}_3(j,t) = -\Delta Da_3(j,t) X_3(j,t) + \alpha[Da_1 e_1(j,t) + Da_2 e_2(j,t)] X_3^2(j,t), \tag{30}$$

on introducing space-time dependence in the chosen response parameter, i.e., $\hat{D}a_3(j,t)$ with $Da_3(j,0) = \hat{D}a_3$. As before, we now define a new variable, $\Delta Da_3(j,t)$, for the parametric corrections required to be made to the response parameter $\hat{D}a_3$ such that the

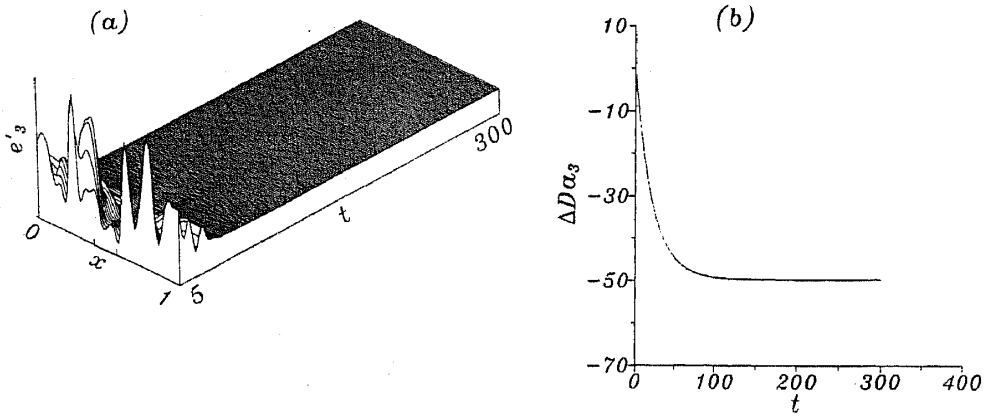

Figure 7. Stabilization of the spatiotemporal chaos with noise reduction. (**a**) The relative error $e'_3(j,t) \to 0$ indicating stabilization of the response system at the desired state; e'_3 axis-scale: (−2.88, 27.89). (**b**) The convergence of $\langle \Delta Da_3 \rangle$ to the initial difference $Da_3 - \hat{D}a_3 = -50$.

true process value Da_3 is realized as $t \to \infty$. For convenience, we assign at $t = 0$, $\Delta Da_3(j,0) = 0$ and to bring out the flexibility in choosing a dynamical form for the parametric self-adaptation, we now consider

$$\frac{\mathrm{d}\Delta Da_3(j,t)}{\mathrm{d}t} = [\hat{X}_3(j,t) - X_3(j,t)]X_3(j,t) = e_3(j,t)X_3(j,t). \tag{31}$$

Then, for a positive Lyapunov functional L defined as

$$L = \sum_i \sum_j e_i^2(j,t) + \sum_j \Delta Da_3^2(j,t), \tag{32}$$

its derivative, $\dot{L}$, is again seen to be strictly nonpositive and from the Lyapunov stability theorem it follows that the response system would completely synchronize with the stable process dynamics for appropriate dynamic corrections, $\Delta Da_3(j,t)$. This was also numerically confirmed for noisy driving signals, $X'_3(k,t)$, from a sub-system of the process. However, unlike in the previous studies, we now observe synchronization over the entire spatial domain. This is clearly seen in figure 7a for the relative error signal, $e'_3(j,t) \to 0, j = 1,\ldots,N$, when the response system was assumed to be driven by time-series signals from a sub-system of size $n_s = 11$, from the central region of the process (following (27)), viz., $X'_3(k,t)$, $k = 1,2,\ldots,n_s$. As in the previous study, for the lattice sites outside the sub-system (and not covered by (31)), an average adaptation $\langle \Delta Da_3 \rangle = \sum_k \Delta Da_3(k,t)/n_s$ was employed. The convergence of $\langle \Delta Da_3 \rangle$ to the initial difference in the response and process parameters, $Da_3 - \hat{D}a_3 = -50$, is seen in figure 7b. Similar results were observed on varying the noise strength γ. Thus, the self-adaptation mechanism can be effectively used even in the presence of reasonable extents of noise. These results also suggest that it may be possible to stabilize the spatiotemporal chaos in real-life experiments, using only scalar driving signals from a subsystem of an experimental process along with an appropriate self-adaptation mechanism as controller feedback. Importantly, a knowledge of the nonlinear mathematical model or a process simulator may not be essential.

4.4 *Multi-parameter control*

In the different situations discussed above, inaccuracies were assumed in only a single system parameter. However in many situations, the inaccuracies may exist in more than one parameter and for synchronization to occur, simultaneous correction in all the inaccurate parameters would then be required. This topic is being actively pursued and different strategies, e.g., parametric self-adaptation [64, 66], optimization [68], neural networks [69, 70], etc. have been reported. In this subsection, we show that multi-parameter control of a spatiotemporally chaotic system via judicious self-adaptation is feasible and advantageous because of its simplicity. For the sake of convenience, we rewrite the process equations as

$$\begin{aligned}
\dot{X}_1(j,t) =& 1 - X_1(j,t) - Da_1 X_1(j,t) X_3^2(j,t) \\
&+ D_1[X_1(j+1,t) - 2X_1(j,t) + X_1(j-1,t)], \\
\dot{X}_2(j,t) =& \beta - X_2(j,t) - Da_2 X_2(j,t) X_3^2(j,t) \\
&+ D_2[X_2(j+1,t) - 2X_2(j,t) + X_2(j-1,t)], \\
\dot{X}_3(j,t) =& A_1 - A_2 X_3(j,t) + A_3[Da_1 X_1(j,t) + Da_2 X_2(j,t)] X_3^2(j,t) \\
&+ D_3[X_3(j+1,t) - 2X_3(j,t) + X_3(j-1,t)],
\end{aligned} \tag{33}$$

where A_1, A_2, and A_3 are the chosen control parameters and may be identified as $A_1 = 1.0$, $A_2 = 1 + Da_3 = 81$, and $A_3 = \alpha = 1.5$ in (3). Let us assume that these are incorrectly set to $\hat{A}_1 = 1.1$, $\hat{A}_2 = 82$, and $\hat{A}_3 = 1.7$, respectively, in the response system driven by the time-series signals, $X_3(j,t)$, $j = 1, 2, \ldots, N$. Thus,

$$\begin{aligned}
\dot{\hat{X}}_1(j,t) =& 1 - \hat{X}_1(j,t) - Da_1 \hat{X}_1(j,t) X_3^2(j,t) \\
&+ D_1[\hat{X}_1(j+1,t) - 2\hat{X}_1(j,t) + \hat{X}_1(j-1,t)], \\
\dot{\hat{X}}_2(j,t) =& \beta - \hat{X}_2(j,t) - Da_2 \hat{X}_2(j,t) X_3^2(j,t) \\
&+ D_2[\hat{X}_2(j+1,t) - 2\hat{X}_2(j,t) + \hat{X}_2(j-1,t)], \\
\dot{\hat{X}}_3(j,t) =& \hat{A}_1 - \hat{A}_2 X_3(j,t) + \hat{A}_3[Da_1 \hat{X}_1(j,t) + Da_2 \hat{X}_2(j,t)] X_3^2(j,t) \\
&+ D_3[X_3(j+1,t) - 2X_3(j,t) + X_3(j-1,t)].
\end{aligned} \tag{34}$$

The aim is then to control the response system dynamics by proper estimation of the parametric corrections, viz., ΔA_1, ΔA_2 and ΔA_3. We first show that for an appropriate choice of driving signals and functional forms for self-adaptation, a Lyapunov functional may be formulated to assess the synchronization and control capability of the response system. The dynamical behaviour of the error functions, $e_i(j,t) = \hat{X}_i(j,t) - X_i(j,t)$, is

$$\begin{aligned}
\dot{e}_1(j,t) =& -e_1(j,t)[1 + Da_1 X_3^2(j,t)] \\
&+ D_1[e_1(j-1,t) - 2e_1(j,t) + e_1(j+1,t)],
\end{aligned} \tag{35}$$

$$\begin{aligned}
\dot{e}_2(j,t) =& -e_2(j,t)[1 + Da_2 X_3^2(j,t)] \\
&+ D_2[e_2(j-1,t) - 2e_2(j,t) + e_2(j+1,t)],
\end{aligned} \tag{36}$$

$$\dot{e}_3(j,t) = \Delta A_1(j,t) - \Delta A_2(j,t)X_3(j,t) + Da_1[\Delta A_3(j,t)\hat{X}_1(j,t) + A_3 e_1(j,t)]X_3^2(j,t) + Da_2[\Delta A_3(j,t)\hat{X}_2(j,t) + A_3 e_2(j,t)]X_3^2(j,t), \quad (37)$$

with the dynamical equations for the parametric corrections, $\Delta A_i(j,t)$, $i = 1,2,3$, chosen respectively, as

$$\dot{\Delta}A_1(j,t) = -[\hat{X}_3(j,t) - X_3(j,t)] = -e_3(j,t), \quad (38)$$

$$\dot{\Delta}A_2(j,t) = [\hat{X}_3(j,t) - X_3(j,t)]X_3(j,t) = e_3(j,t)X_3(j,t), \quad (39)$$

$$\dot{\Delta}A_3(j,t) = -Da_1\hat{X}_1(j,t)[\hat{X}_3(j,t) - X_3(j,t)]X_3^2(j,t) - Da_2\hat{X}_2(j,t)[\hat{X}_3(j,t) - X_3(j,t)]X_3^2(j,t) = [Da_1\hat{X}_1(j,t) + Da_2\hat{X}_2(j,t)]e_3(j,t)X_3^2(j,t). \quad (40)$$

Then the derivative of a positive Lyapunov functional, $L = \sum_i \sum_j [e_i^2(j,t) + \Delta A_i^2(j,t)]$, is

$$(1/2)\dot{L} = \sum_i \sum_j [e_i(j,t)\dot{e}_i(j,t) + \Delta A_i(j,t)\dot{\Delta}A_i(j,t)], \quad (41)$$

that is,

$$(1/2)\dot{L} = -\sum_{j=1}^{N}\{e_1^2(j,t)[1 + Da_1X_3^2(j,t)] - D_1[e_1(j,t) - e_1(j+1,t)]^2\} - \sum_{j=1}^{N}\{e_2^2(j,t)[1 + Da_2X_3^2(j,t)] - D_2[e_2(j,t) - e_2(j+1,t)]^2\} + \sum_{j=1}^{N} A_3 e_3(j,t)[Da_1e_1(j,t) + Da_2e_2(j,t)]X_3^2(j,t). \quad (42)$$

It may be noted that (35) and (36) are again decoupled systems, and following the arguments presented in the previous subsections, we obtain $e_i(j,t) \to 0$ as $t \to \infty$, for $i = 1,2$. Using these results in (41), it is clear that $\dot{L}$ is non-positive and dynamical synchronization of the response with the process should be possible. This was confirmed numerically and below we present our results obtained on using driving signals only from a sub-system of the process, i.e., in $X_3(k,t)$, $k = 1,2,\ldots,n_s$. As before, we begin by introducing space-time dependence in the chosen control parameters, and assume that at $t = 0$, $\hat{A}_i(j,0) = \hat{A}_i \neq A_i$. The parametric corrections, $\Delta A_i(k,t)$'s, within the sub-system are assumed to be governed by (38–40). For the lattice sites outside the sub-system, an average adaptation, $\langle \Delta A_i \rangle = \sum_k \Delta A_i(k,t)/n_s$, were implemented. Figures 8a, 8b and 8c respectively show the convergence of $\langle \Delta A_1 \rangle \to -0.1$, $\langle \Delta A_2 \rangle \to -1.0$ and $\langle \Delta A_3 \rangle \to -0.2$, the required corrections. Thus, these results suggest that it may be possible to simultaneously adapt more than one system parameter using limited scalar time-series data from a sub-system of the process for appropriate choices of the functional forms for parametric corrections. It may be clarified that when $n_s = N$, not only adaptation of the parameters but control via synchronization of the complete space-time dynamics of the response system may be possible.

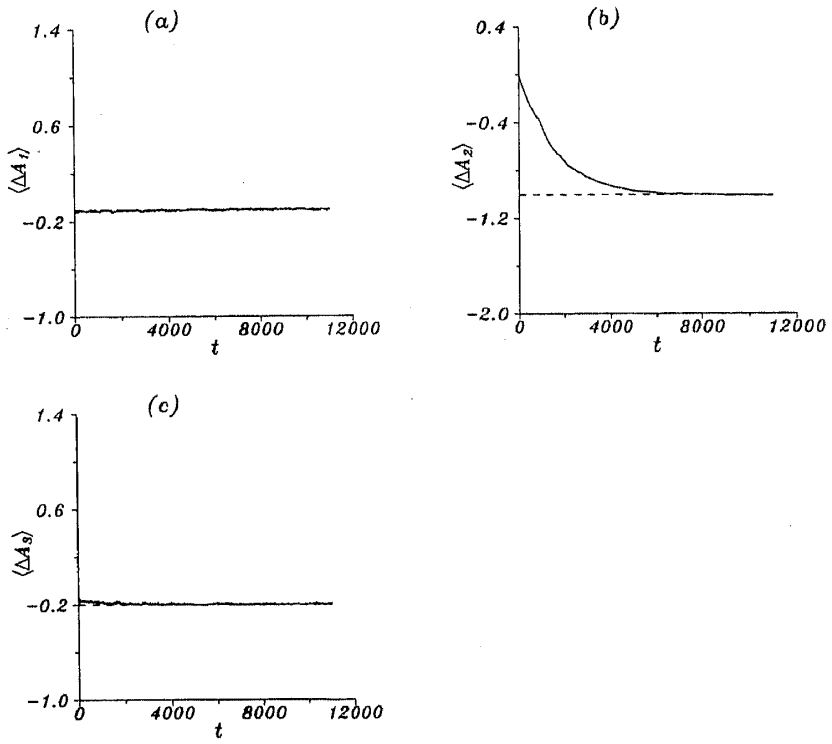

Figure 8. (**a, b, c**) Multi-parameter control via self-adaptation showing the accurate estimation of the corrections, $\langle \Delta A_i \rangle$, $i = 1, 2, 3$.

5. Conclusion

The analysis of sub-system dynamics for a nonlinear autocatalytic reaction-diffusion system as a function of increasing sub-system size showed interesting linear scaling relationships with respect to the invariant measures like the Lyapunov dimension and KS-entropy, while the dimension densities and normalized entropy were found to become independent of the sub-system size beyond a certain critical size n_{sc}. These results suggest that characterization of the complete system dynamics may be possible from an analysis of the Lyapunov spectrum of its sub-system of size $n_s > n_{sc}$ with considerable reduction in the computational effort. Our preliminary results for the autocatalytic reaction-diffusion system on a two-dimensional lattice has also shown similar trends for the system invariants as a function of its sub-system size. Thus, the approach of analyzing sub-system behaviour may be advantageously used in the characterization of more complex higher-dimensional systems. It may be noted that the studies discussed in this paper were carried out for nearest-neighbor diffusive coupling. However, in most practical situations, other transport mechanisms such as convection may also concurrently occur. It would then be worthwhile to study the validity of the scaling relationships in the sub-system invariant properties for systems involving more complex and long-range coupling.

We have used the above characterization results to analyse the synchronization and controllability of spatiotemporal systems exhibiting chaotic dynamics. The control objectives were carried out for inaccurate knowledge of the initial conditions, parameter

settings, and limitations in the monitoring of time-series data from the spatial domain which may additionally be corrupted with noise. Our results using sub-system information show that it may be possible to correctly estimate the inaccuracies in the control parameter(s) via suitably chosen forms of parametric self-adaptation(s). Suppression of chaos and stabilization of the spatiotemporally chaotic dynamics to a desired stable state was also possible using sub-system driving signals even in the presence of reasonable extents of noise. However, for the synchronization of complex and chaotic dynamics, time-series data from the entire spatial domain may be required. Further, it has been shown that it may be possible to assess the synchronization capability of a spatiotemporal system from the stability analysis of suitably constructed Lyapunov functionals. This approach offers the advantage of *a priori* knowledge of the synchronization behaviour under different situations.

Acknowledgements

The authors gratefully acknowledge the financial support of the Department of Science and Technology, New Delhi in carrying out this work.

References

[1] M C Cross and P C Hohenberg, *Rev. Mod. Phys.* **65**, 851 (1993)
[2] Y C Lai and R L Winslow, *Physica* **D74**, 353 (1994)
[3] T Shinbrot, *Nonlinear Science Today* **3**, 1 (1993)
[4] H Gang and H Kaifen, *Phys. Rev. Lett.* **71**, 3794 (1993)
[5] E Kostelich, C Grebogi, E Ott and J A Yorke, *Phys. Rev.* **E47**, 305 (1993)
[6] D Auerbach, *Phys. Rev. Lett.* **72**, 1184 (1994)
[7] L Poon and C Grebogi, *Phys. Rev. Lett.* **75**, 4023 (1995)
[8] A Karma, *Phys. Rev. Lett.* **71**, 1103 (1993)
[9] M Bär and M Eiswirth, *Phys. Rev.* **E48**, R1635 (1993)
[10] R Imbihl and G Ertl, *Chem. Rev.* **95**, 697 (1995)
[11] B I Shraiman *et al*, *Physica* **D57**, 241 (1992)
[12] I Aranson, L Aranson, L Kramer and A Weber, *Phys. Rev.* **A46**, 2992 (1992)
[13] I Aranson, H Levine and L Tsimring, *Phys. Rev. Lett.* **72**, 2561 (1994)
[14] J F Lindner, B K Meadows, W L Ditto, M E Inchiosa and A R Bulsara, *Phys. Rev. Lett.* **75**, 3 (1995)
[15] Y Braiman, J F Lindner and W L Ditto, *Nature* (*London*) **378**, 465 (1996)
[16] H D I Abarbanel, R Brown, J J Sidorowich and L Tsimring, *Rev. Mod. Phys.* **65**, 1331 (1993)
[17] H Fujisaka and T Yamada, *Prog. Theor. Phys.* **69**, 32 (1983)
[18] L M Pecora and T L Carroll, *Phys. Rev. Lett.* **64**, 821 (1990)
[19] L M Pecora and T L Carroll, *Phys. Rev.* **A44**, 2374 (1991)
[20] R He and P G Vaidya, *Phys. Rev.* **A46**, 7387 (1992)
[21] K M Cuomo and A V Oppenheim, *Phys. Rev. Lett.* **71**, 65 (1993)
[22] M Ding and E Ott, *Phys. Rev.* **E49**, R945 (1994)
[23] C W Wu and L O Chua, *Int. J. Bifur. Chaos* **4**, 979 (1994)
[24] J F Heagy, T L Carroll and L M Pecora, *Phys. Rev.* **E50**, 1874 (1994)
[25] N F Rulkov, M M Sushchik, L S Tsimring and H D I Abarbanel, *Phys. Rev.* **E51**, 980 (1995)
[26] L Kocarev and U Parlitz, *Phys. Rev. Lett.* **76**, (1996)
[27] T C Newell, P M Alsing, A Gavrielides and V Kovanis, *Phys. Rev. Lett.* **72**, 1647 (1994)
[28] T C Newell, P M Alsing, A Gavrielides and V Kovanis, *Phys. Rev.* **E49**, 313 (1994)
[29] E Ott, C Grebogi and J A Yorke, *Phys. Rev. Lett.* **64**, 1196 (1990)

[30] Y C Lai and C Grebogi, *Phys. Rev.* **E47**, 2357 (1993)
[31] P Grassberger, *Phys. Scr.* **40**, 346 (1989)
[32] G Mayer-Kress and K Kaneko, *J. Stat. Phys.* **54**, 1489 (1989)
[33] A Torcini, A Politi, G Puccioni and G Alessandro, *Physica* **53**, 85 (1991)
[34] H Chate, G Grinstein and L H Tang, *Phys. Rev. Lett.* **74**, 912 (1995)
[35] M Bauer, H Heng and W Martienssen, *Phys. Rev. Lett.* **71**, 521 (1993)
[36] N Parekh, V Ravi Kumar and B D Kulkarni, (submitted)
[37] Y C Lai and C Grebogi, *Phys. Rev.* **E52**, 1894 (1994)
[38] J Warncke, M Bauer and W Martienssen, *Europhys. Lett.* **25**, 323 (1994)
[39] J H Peng, E J Ding, M Ding and W Yang, *Phys. Rev. Lett.* **76**, 904 (1996)
[40] N Parekh, V Ravi Kumar and B D Kulkarni, *Physica* **A224**, 369 (1996)
[41] V Castets, E Dulos, J Boissonade and P De Kepper, *Phys. Rev. Lett.* **64**, 2953 (1990)
[42] Y Kuramoto, *Chemical oscillations, waves and turbulence* (Berlin: Springer) (1984)
[43] G Nicolis, *J. Phys.* **C2**, SA47 (1990)
[44] W Ouyang and H L Swinney, *Nature* (*London*) **352**, 610 (1991)
[45] P Gray and S Scott, *Chem. Eng. Sci.* **38**, 29 (1983)
[46] J E Pearson, *Science* **261**, 189 (1993)
[47] K J Lee, W D McCormick, J E Pearson and H L Swinney, *Nature* (*London*) **369**, 215 (1994)
[48] N Parekh, V Ravi Kumar and B D Kulkarni, *Phys. Rev.* **E52**, 5100 (1995)
[49] D T Lynch, *Chem. Engg. Sci.* **47**, 4435 (1992)
[50] D Horváth, Valery Petrov, S K Scott and K Showalter, *J. Chem. Phys.* **98**, 6332 (1993)
[51] V Petrov, S K Scott and K Showalter, *Philos. Trans. R. Soc. London* **A347**, 631 (1994)
[52] J Argyris, G Faust and M Haase, *An exploration of chaos* (Elsevier Science B V, Amsterdam, 1994)
[53] J L Kaplan and J A Yorke, *Lecture notes in mathematics* **730**, 204 (1979)
[54] S N Rasband, *Chaotic dynamics of nonlinear systems* (Wiley-Interscience, 1989)
[55] Y B Pesin, *Russ. Math. Sur.* **32**, 55 (1977)
[56] H Tong, *Nonlinear time series: A dynamical system approach* (Clarendon Press, Oxford, 1990)
[57] B A Huberman and E Lumer, *IEEE Trans. Circuits Syst.* **37**, 547 (1990)
[58] S Sinha and R Ramaswamy, *Physica* **D43**, 118 (1990)
[59] V Ravi Kumar, B D Kulkarni and P B Deshpande, *Proc. R. Soc. London Ser.* **A433**, 711 (1991)
[60] S Rajashekar and M Lakshmanan, *Int. J. Bifur. Chaos* **2**, 201 (1992)
[61] K Pyragas, *Phys. Lett.* **A181**, 203 (1993)
[62] J K Bandyopadhyay, V Ravi Kumar, B D Kulkarni and P Bhattacharya, *Chem. Engg. Sci.* **48**, 3545 (1993)
[63] H K Qammer, F Mossayebi and L Murphy, *Phys. Lett.* **A178**, 279 (1993)
[64] D Vassiliadis, *Physica* **D71**, 319 (1994)
[65] J K John and R E Amritkar, *Phys. Rev.* **E49**, 4843 (1994)
[66] U Pralitz, *Phys. Rev. Lett.* **76**, 1232 (1996)
[67] H G Bock, *Progress in scientific computing* (Birkhäuser, Boston) **2**, 95 (1983)
[68] E Baake, M Baake, H G Bock and K M Briggs, *Phys. Rev.* **A45**, 5524 (1992)
[69] J C Principe, A Rathie and J M Huo, *Int. J. Bifur. Chaos* **2**, 989 (1992)
[70] S A Billings and S Chen, *Neural networks and system identification* (Peter Peregrinus, London, 1992) p. 181